Electronic Supplementary Information

Structures and magnetic properties of several phenoxo-O bridged dinuclear lanthanide complexes: Dy derivatives displaying substituent dependent magnetic relaxation behavior

Wen-Min Wang,[a,b] Wan-Zhen Qiao,[b] Hong-Xia Zhang,[a] Shi-Yu Wang,[a] Yao-Yao Nie,[a] Hong-Man Chen,[a] Zhen Liu,[a] Hong-Ling Gao,[a] Jian-Zhong Cui*[a] and Bin Zhao*[b]

.

~~Table S1.~~ ~~The important bond~~ lengths (Å)and angles (°) for **1**–**9**.

[a]*Department of Chemistry, Tianjin University, Tianjin, 300072, China. E-mail:* cuijianzhong@tju.edu.cn (J.-Z. Cui).

[b] *Department of Chemistry, Key Laboratory of Advanced Energy Material Chemistry, MOE, TKL of Metal and Molecule Based Material Chemistry, and Collaborative Innovation Center of Chemical Science and Engineering (Tianjin), Nankai University, Tianjin 300071, China.* zhaobin@nankai.edu.cn. (B. Zhao)

Complexes	The range of Ln–O bond lengths / Å	Average Ln–O bond lengths / Å	The distance of Ln---Ln / Å	The Ln–O–Ln bond angles /°
1	2.330(4)–2.444(3)	2.375(5)	3.943(0)	109.66(1) and 109.64(1)
2	2.306(4)–2.408(3)	2.346(4)	3.848(0)	107.96(1) and 108.71(1)
3	2.282(4)–2.389(4)	2.334(4)	3.840(5)	108.56(1)
4	2.265(1)–2.374(0)	2.320(2)	3.819(1)	108.85(6)
5	2.261(5)–2.355(5)	2.307(7)	3.801(2)	109.28(1)
6	2.306(8)–2.426(8)	2.343(8)	3.875(0)	108.63(0)
7	2.300(3)–2.403(3)	2.328(3)	3.861(2)	109.39(1)
8	2.299(6)–2.391(8)	2.320(4)	3.841(5)	109.43(5)
9	2.279(2)–2.376(2)	2.307(4)	3.829(0)	109.47(8)

Table S2. The parameters ***C*** and ***θ*** of **2-9** was generated from the best fit by the Curie-Weiss expression.

	2	**3**	**4**	**5**	**6**	**7**	**8**	**9**
C / cm^3 K mol^{-1}	24.28	28.77	28.55	23.70	24.00	28.16	28.16	23.76
θ/K	-7.72	-5.03	-6.52	-9.20	-3.75	-6.19	-7.25	-8.63

Table S3. The continuous symmetry measurement value calculated by SHAPE 2.0 for complexes **3** and **7**.

Dy^{3+}	D_{4d}SAPR	D_{2d}TDD	C_{2v}JBTPR	C_{2v}BTPR	D_{2d}JSD
Complex **3**	2.371	0.853	3.348	2.380	3.636
Complex **7**	3.389	0.821	3.562	2.671	3.462

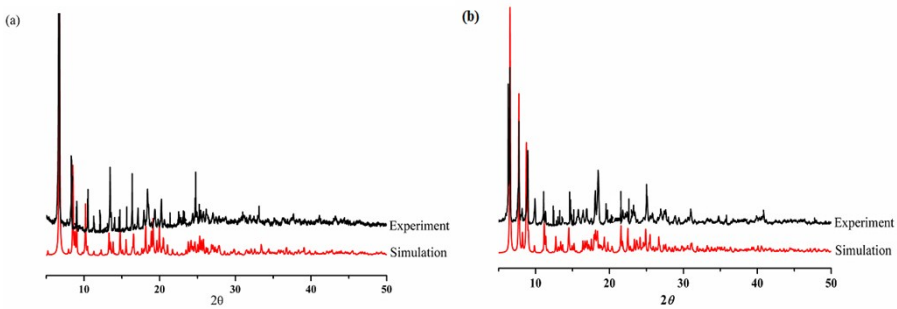

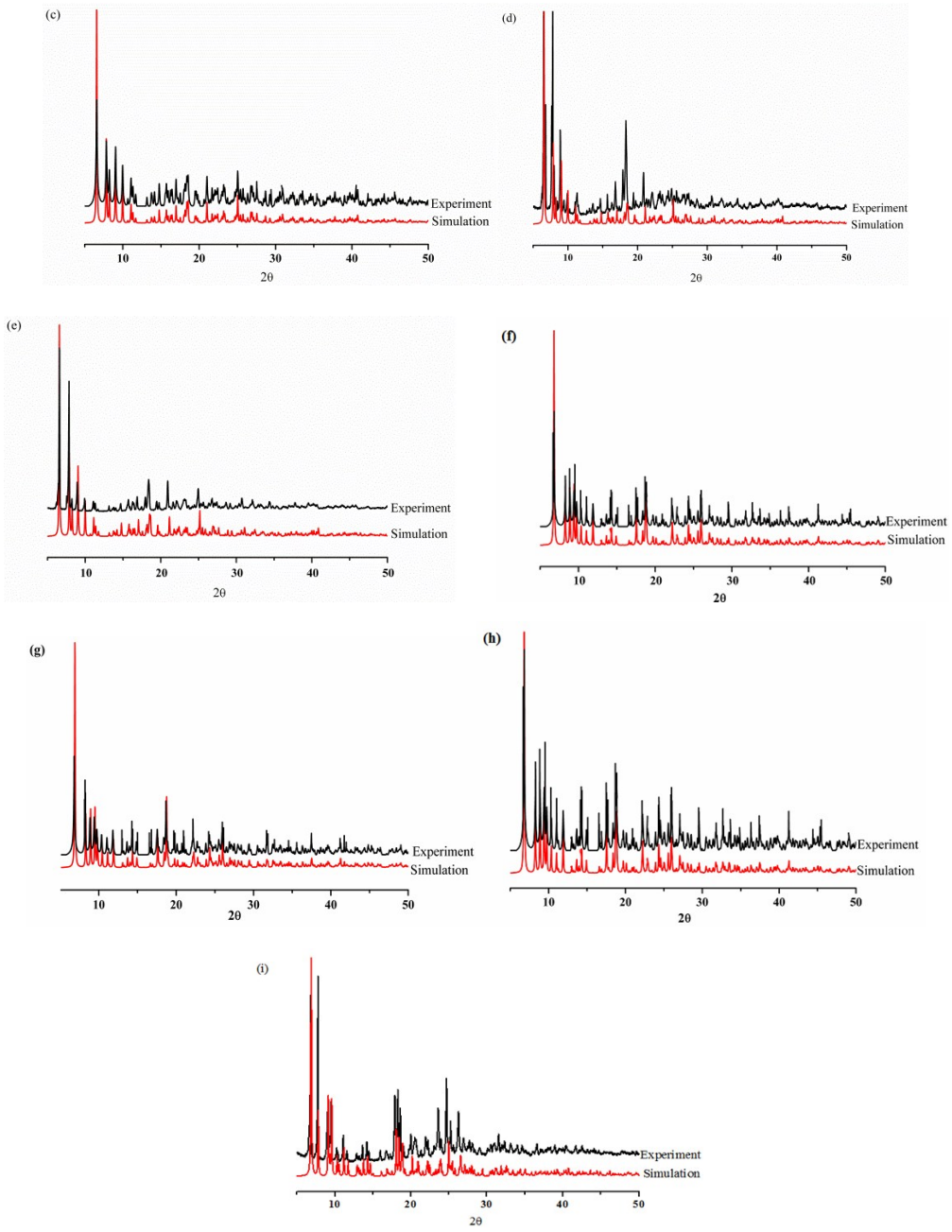

Fig. S1 PXRD patterns for **1** (a)**, 2** (b), **3** (c), **4** (d), **5** (e), **6** (f), **7** (g), **8** (h) and **9** (i)**.**

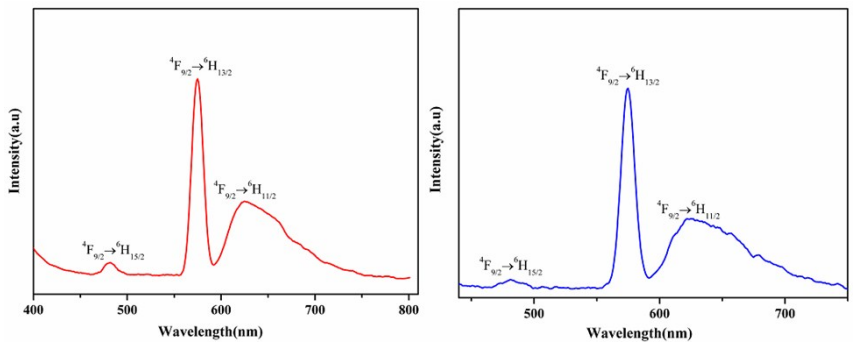

Fig. S2 The solid-state luminescence spectrums of **3** (left) and **7** (right) at room temperature.

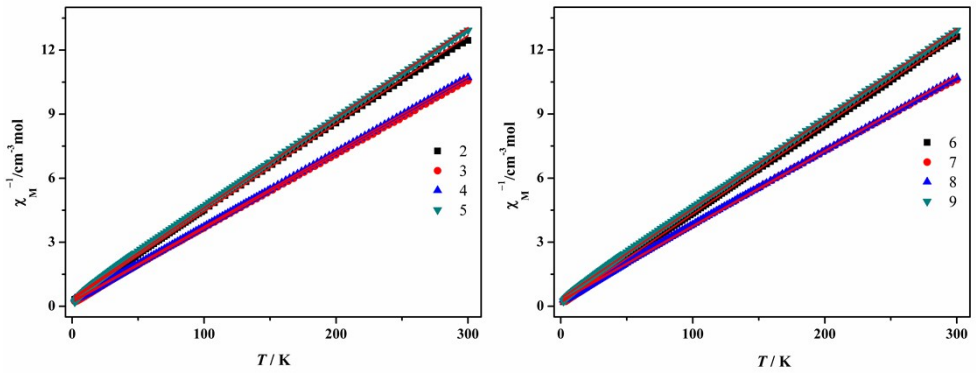

Fig. S3 Temperature dependence of the magnetic susceptibility in the form of χ_M^{-1} vs *T* for **2-5**(left) and **6-9**(right) at an applied field of 1000 Oe between 2 and 300 K. The solid line was generated from the best fit by the Curie-Weiss expression.

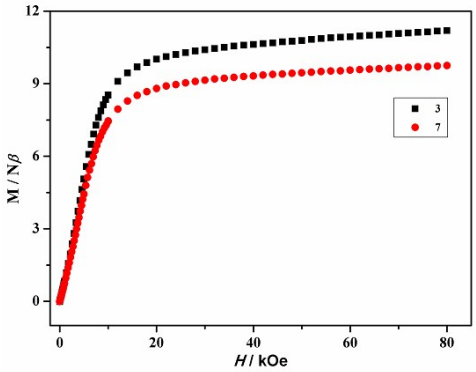

Fig. S4 *M vs. H* plots for **3** and **7** at 2 K.

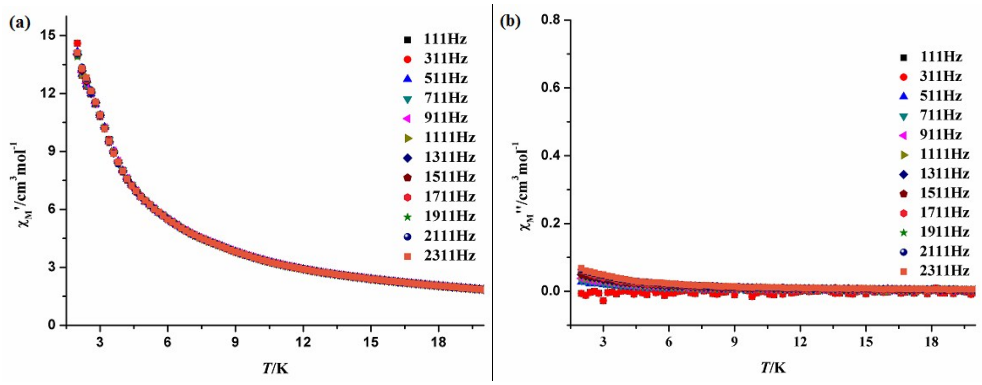

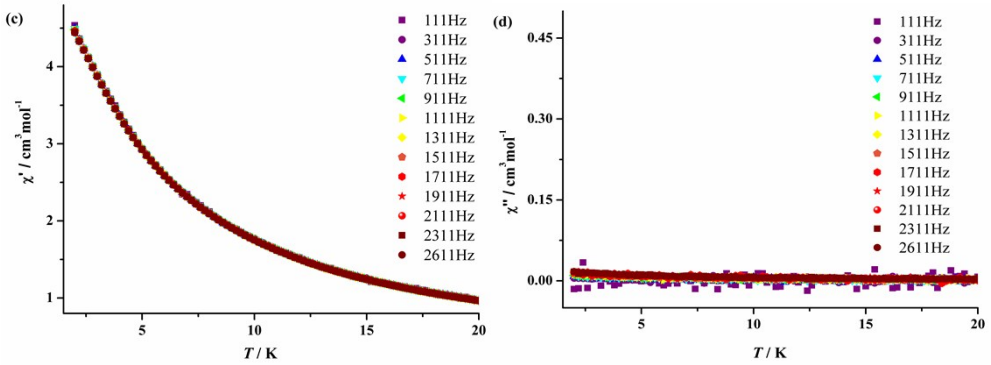

Fig. S5 Temperature dependence of the in-phase (left) and out-of-phase (right) components of the *ac* magnetic susceptibility for **2 (**a and b**)** and **6** (c and d) in zero dc fields with an oscillation of 3.0 Oe.

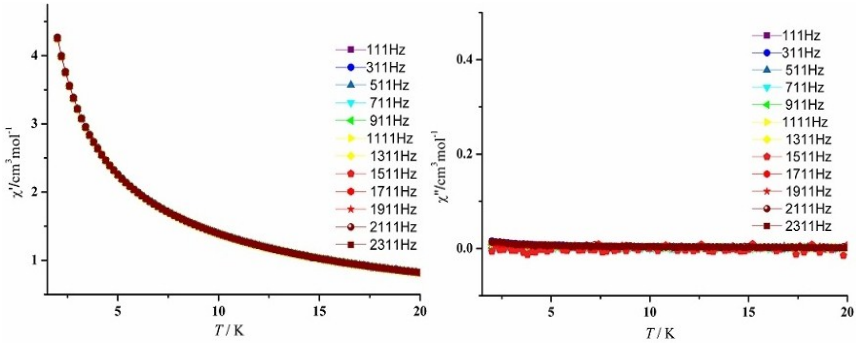

Fig. S6 Temperature dependence of the in-phase (χ′) and out-of-phase (χ″) components of the ac magnetic susceptibility for **5** in zero dc fields with an oscillation of 3.0 Oe.

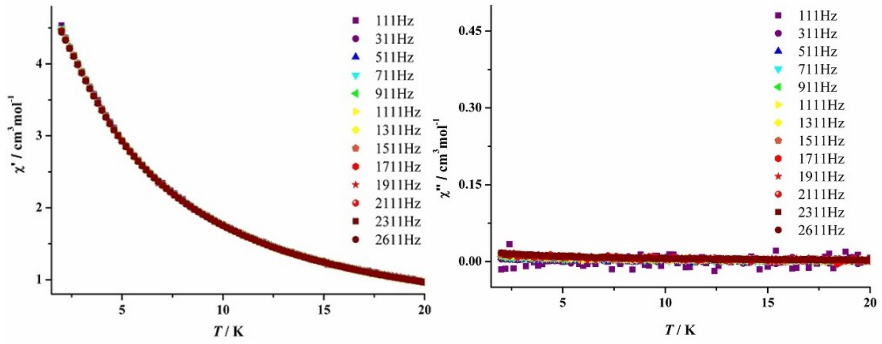

Fig. S7 Temperature dependence of the in-phase (χ′) and out-of-phase (χ″) components of the ac magnetic susceptibility for **9** in zero dc fields with an oscillation of 3.0 Oe.

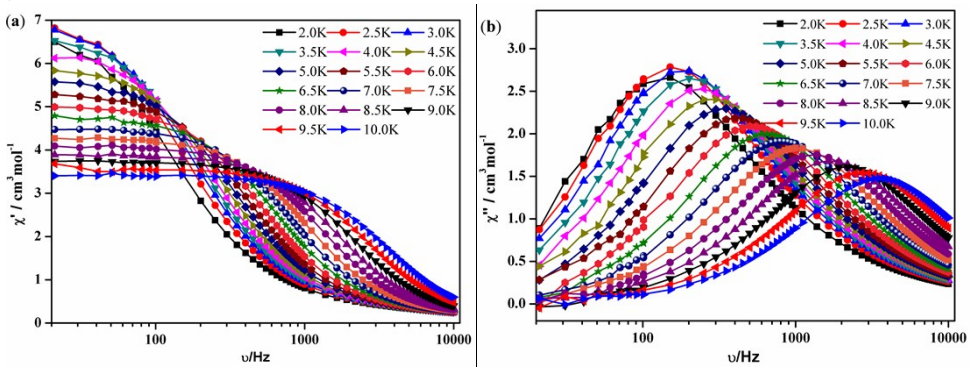

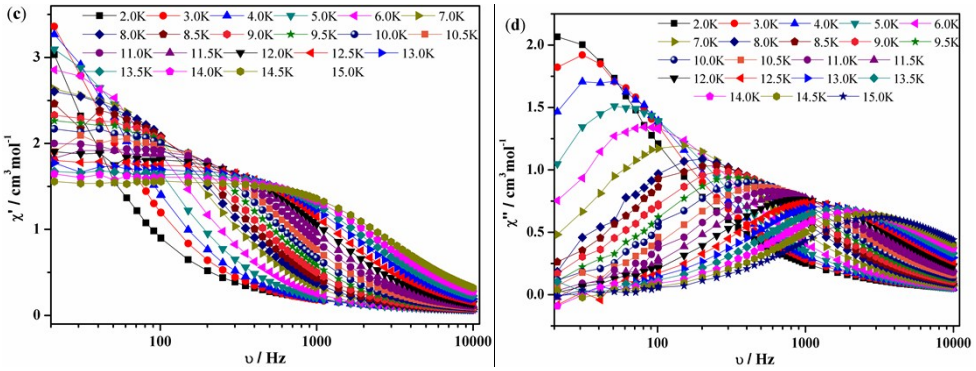

Fig. S8 Frequency dependence of the in-phase (χ′) and out-of-phase (χ″) ac susceptibility for **3** (a and b) and **7** (c and d) under zero dc field.